

# Dopamine Transporter Imaging with Fluorine-18-FPCIT and PET

Ken Kazumata, Vijay Dhawan, Thomas Chaly, Angelo Antonini, Claude Margouleff, Abdelfatihe Belakhlef, John Neumeyer and David Eidelberg

Departments of Neurology and Research, North Shore University Hospital, Manhasset; New York University School of Medicine, New York, New York; Department of Psychiatry, McLean Hospital, Belmont; and Harvard Medical School, Boston, Massachusetts

Fluorinated N-3-fluoropropyl-2- $\beta$ -carboxymethoxy-3- $\beta$ -(4-iodophenyl) nortropane (FPCIT) has been synthesized as a dopamine transporter ligand for PET studies. We evaluated the regional brain uptake and the plasma metabolism of [ $^{18}\text{F}$ ]-FPCIT. **Methods:** PET studies were conducted on 7 normal subjects and on 10 patients with Parkinson's disease. After the [ $^{18}\text{F}$ ]-FPCIT injection ( $4.4 \pm 1.8$  mCi), dynamic scans were acquired over 100 min. Plasma metabolite analysis was performed using high-performance liquid chromatography (HPLC). **Results:** Plasma HPLC revealed two peaks corresponding to unmetabolized [ $^{18}\text{F}$ ]-FPCIT and a polar metabolite. The fraction of the parent compound decreased rapidly to 25% at 25 min. Fluorine-18-FPCIT showed a striatum-to-occipital ratio (SOR) of 3.5 at 90 min postinjection. The ratio of striatal-to-occipital distribution volume (DVR) was calculated directly by using a mean tissue-to-plasma efflux constant for occipital cortex obtained in 10 subjects ( $k_2 = 0.037 \text{ min}^{-1}$ ). DVR measures determined with and without plasma input function were correlated ( $r = 0.98$ ,  $p < 0.0001$ ). In normal subjects, a significant age-related decline of DVR was observed both for caudate and putamen, corresponding to a 7.7% and 6.4% decline per decade, respectively ( $r > 0.85$ ,  $p < 0.01$ ). Both DVR and SOR correctly classified early-stage Parkinson's disease patients with comparable accuracy ( $p < 0.0001$ ). Age-corrected DVR values correlated negatively with the Uniform Parkinson's Disease Rating Scale composite motor ratings ( $r = 0.66$ ,  $p < 0.05$ ). **Conclusion:** The tracer characteristics are compatible with a high-affinity, reversible ligand. FPCIT/PET demonstrated age-related decline in dopamine transporter binding in normal subjects as well as significant reductions in patients with idiopathic Parkinson's disease, which correlates with the disease severity.

**Key Words:** fluorine-18-fluorinated N-3-fluoropropyl-2- $\beta$ -carboxymethoxy-3- $\beta$ -(4-iodophenyl) nortropane; PET; dopamine transporter; Parkinson's disease; aging effect

J Nucl Med 1998; 39:1521-1530

An N- $\omega$ -fluoroalkyl analog of  $\beta$ -CIT, (N-3-fluoropropyl-2- $\beta$ -carboxymethoxy-3- $\beta$ -(4-iodophenyl) nortropane) (FPCIT) has been developed for imaging dopamine transporter (DAT) binding in vivo (1,2). Because the dopamine transporter is localized to the presynaptic terminal, DAT binding can serve as a marker of dopaminergic function (3-9). Importantly, radiolabeled  $\beta$ -CIT analogs can afford the possibility of comparative PET and SPECT studies using molecularly identical tracers. This development may expand significantly the role of quantitative imaging in clinical research in parkinsonism (6,10). Recent investigations with [ $^{11}\text{C}$ ]- and [ $^{123}\text{I}$ ]-labeled FPCIT have demonstrated faster kinetics as well as higher DAT selectivity than  $\beta$ -CIT (1,2,11-14).

In a previous study, we found that SPECT imaging with

[ $^{123}\text{I}$ ]-FPCIT differentiated Parkinson's disease patients from normal volunteers with the same accuracy obtained by 6-[ $^{18}\text{F}$ ]fluorodopa (FDOPA) and PET (9). In contrast to FDOPA PET,  $\beta$ -CIT and FPCIT SPECT studies have shown a decline of dopaminergic function with normal aging (9,15). In addition to measuring different aspects of dopaminergic function, DAT imaging also may have an advantage over FDOPA for several reasons. (a) FDOPA quantifies the activity of dopa decarboxylase (DDC), which might be maintained at high levels in residual dopaminergic neurons (16,17). Concomitantly, DAT activity may be downregulated in Parkinson's disease, especially in drug-naïve patients; (b) Transport of 3OMD across the blood brain barrier can affect the quantification of DDC activity, thus confounding results achieved with FDOPA PET (18-20); and (c) signal to noise is potentially higher for DAT imaging than for FDOPA PET (1,2,13).

Recently, we synthesized [ $^{18}\text{F}$ ]-FPCIT as a new PET ligand for imaging DAT activity (21). In the current study, we evaluated the regional brain uptake of [ $^{18}\text{F}$ ]-FPCIT in healthy human volunteers and in patients with Parkinson's disease. We performed plasma high-performance liquid chromatography (HPLC) analysis in each PET study to estimate the contributions of the metabolites to the arterial input function. Graphical analysis was applied to obtain volume of distribution and the ratio of striatal distribution volume to that of an occipital reference region (22,23). We also investigated the correlations of the PET measurements with objective clinical measurements of nigrostriatal function in normal aging and parkinsonism.

## MATERIALS AND METHODS

### Subjects

We recruited 10 idiopathic Parkinson's disease patients without dementia (3 women, 7 men; age range  $63.1 \pm 11.0$  yr; mean  $\pm$  s.d.) from the Movement Disorders Center of North Shore University Hospital, Manhasset, NY. Patients were selected with mild-to-moderate stage Parkinson's disease [Hoehn and Yahr (H&Y) Stage I ( $n = 7$ ); II ( $n = 2$ ); III ( $n = 1$ )]. Three patients were newly diagnosed and previously untreated with dopaminergic therapy. A diagnosis of Parkinson's disease was made if the patients had pure parkinsonism without a history of known causative factors such as encephalitis or neuroleptic treatment or did not have early dementia, supranuclear gaze palsy or ataxia. In all patients, family history was negative for neurodegenerative illnesses. Permission was obtained from the Institutional Review Board of North Shore University Hospital to perform the studies. Written consent for all subjects was obtained after a detailed explanation of the scanning procedures. The clinical characteristics of these patients are presented in Table 1.

We also recruited 7 normal volunteer subjects (5 women, 2 men; age range 23-73 yr; mean  $50.8 \pm 19.4$  yr) by soliciting hospital personnel at North Shore University Hospital and the spouses of

Received Aug. 5, 1997; revision accepted Nov. 24, 1997.

For correspondence or reprints contact: David Eidelberg, MD, Department of Neurology, North Shore University Hospital, 350 Community Drive, Manhasset, New York, 11030.

**TABLE 1**  
Characteristics of Parkinson's Disease Patients

Patient No.	Age (yr)	Sex	Duration (yr)	H&Y*	UPDRS ratings†				Medication‡
					BK	T	R	Composite	
1	72	M	3	1	1	2	0	3	2
2	45	F	2	1	0	4	0	4	None
3	69	M	10	1	0	2	1	3	1, 2, 3
4	68	M	4	1	0	0	0	2	1, 2, 4
5	65	M	2	1	5	1	0	6	None
6	65	M	3	1	0	2	0	2	1
7	56	M	9	1	1	4	1	8	1
8	75	F	2	2	0	5	0	5	None
9	48	F	12	2	4	4	4	12	2, 3
10	63	M	21	3	13	13	6	44	1, 3, 4

\*Hoehn and Yahr (H&Y) score determined 12 hr off medications.

†Unified Parkinson's Disease Rating Scale (UPDRS) motor ratings obtained preoperatively 12 hr after discontinuation of medications (BK = bradykinesia; T = tremor; R = rigidity).

‡Medications are signified numerically: 1 = levodopa/carbidopa; 2 = deprenyl; 3 = anticholinergics; 4 = dopamine agonist.

the Parkinson's disease patients in local support groups. The following exclusion criteria were used: (a) past history of neurological or psychiatric illness; (b) prior exposure to neuroleptic agents or drug use; (c) past medical history of hypertension, cardiovascular disease and diabetes mellitus; and (d) abnormal neurological examination.

### Radiochemistry

Fluorine-18-FPCIT was prepared with a two-step procedure that involves the fluorination of 1, 3 propanediol di-p-tosylate and the reaction of fluoropropyl tosylate with nor  $\beta$ -CIT. The kryptofix complex was prepared as described elsewhere (21). Precursor was provided by Research Biochemicals, Inc., Natick, MA. Eighteen milligrams of the 1, 3 propanediol di-p-tosylate in acetonitrile were added the reaction vial containing kryptofix complex and the mixture was heated at 105°C under argon for about 20 min. At the end of the reaction, the solvent was removed by blowing argon. Ten milligrams of the nor  $\beta$ -CIT in N,N-dimethylformamide (DMF) were added, and the reaction mixture was heated again for 30 min at 155°C under argon. The solvent was boiled off by passing argon. The crude product was extracted with methanol and subjected to HPLC purification (Phenomenex Bondacilone 10, C18, 250  $\times$  10 mm, 10- $\mu$ ) using 60:40 phosphoric acid (0.6 g in 600 ml HPLC water) and acetonitrile at 2 ml/min. The product eluted at 19 min was collected, and the solvent was removed completely under vacuum (Rotary-evaporation at 70°C). The product was extracted with 50% sterile ethanol (1 ml  $\times$  2) and was reconstituted with 1 ml L-ascorbic acid and sterile saline (4 ml). The solution then was filtered through a sterile filter (0.22 $\mu$ m). Radiochemical purity was about 98%.

### PET Imaging

All patients and normal volunteers fasted at least 6 hr before PET scanning. All antiparkinsonian medications were discontinued at least 12 hr before PET studies. At the time of PET study, all Parkinson's disease patients were rated quantitatively according to the H&Y scale and the Unified Parkinson's Disease Rating Scale (UPDRS 3.0) (24). PET studies were performed using a whole-body, high-resolution PET scanner (Advance; GE Medical Systems, Milwaukee, WI). The performance characteristics of this instrument have been described elsewhere (25). This 18-ring bismuth germanate tomograph produces 35 slices with 4.2 mm resolution in all directions (FWHM). All studies were performed with the subject's eyes open in a dimly lit room and minimal auditory stimulation.

Patients were positioned in the scanner in a Laitinen stereoadaptor (26) using a three-dimensional laser alignment with the gantry aligned parallel to the orbitomeatal (OM) line. Then, 37–244 MBq (1.0–6.6 mCi) [ $^{18}$ F]-FPCIT (1000 Ci/mmol) in 20–25 ml saline was injected into the antecubital vein over 2.5 min with an automated infusion pump. This slow bolus speed was found tolerable to the subjects who otherwise complained of minor irritation at the injection site due to the minimal alcohol content of the injectate. The coincidence counter on the scanner provided the transit time from injection point to the brain (brain delay). A series of 23 emission scans were obtained from time of injection up to 100 min (two 30-sec, two 1-min, five 2-min, eight 5-min, and six 8-min scans). The initial nine frames (0–13 min) were acquired by a two-dimensional mode to eliminate the scatter effects from extracerebral structures and for accurate determination of the brain delay. The subsequent 14 frames (13–100 min) were acquired in a three-dimensional scan mode.

The time course of plasma  $^{18}$ F radioactivity was determined by radial arterial blood sampling followed by plasma centrifugation. Sixteen 9-sec samples were taken by a precision peristaltic pump followed by discrete samples taken at 3.5, 5, 10, 25, 40, 65, 75, 85 and 100 min postinjection. Because the first 16 arterial samples were collected using a pump, an appropriate smearing correction was applied (27).

### High-Performance Liquid Chromatography Analysis

The details of the HPLC analysis are described elsewhere (21). Six blood samples taken at 5, 10, 25, 40, 65 and 100 min postinjection were centrifuged to separate plasma for HPLC. After centrifugation of samples, plasma (0.5 ml) was removed and mixed with acetonitrile (0.5 ml). The mixture was centrifuged and the supernatant was removed and 1 ml was used for the HPLC separation. The analysis was performed on a phenethyl column (5 $\mu$ , 4.6  $\times$  20 mm) eluted with a mixture of acetonitrile and phosphoric acid. The flow was 1.5 ml/min, and a 1-ml sample loop was used. A chromatography curve-fitting program ("peakfit," Jandal Scientific, San Rafael, CA) was used to separate the peaks and calculate the ratio of area under the curves for [ $^{18}$ F]-FPCIT and its metabolites.

### Image Analysis

Regions of interest (ROIs) were drawn on averaged emission scans representing the activity from 60–100 min postinjection. ROIs were defined interactively with reference to MRIs when available. ROIs for the caudate head, putamen, thalamus, midbrain,

occipital cortex and cerebellum were projected to the dynamic emission scans. A detailed description for this procedure has been reported elsewhere (9). Quantitative analysis were performed by using the graphical and the ratio method.

### Graphical Method

Regional time-activity curves were analyzed graphically according to:

$$\frac{\int \text{ROI}(t')dt'}{\text{ROI}(T)} = \frac{\text{DV} \times \int \text{Cp}(t')dt'}{\text{ROI}(T)} + \text{intercept}, \quad \text{Eq. 1}$$

where ROI(T) is tissue radioactivity at  $t' = T$  and DV is the distribution volume (22). Because we did not measure the plasma protein binding, the estimated DV refers to the total arterial tracer. The occipital lobe was used a reference region. According to Logan et al. (23), the ratio of striatal to occipital DV (DVR) is provided by the regression slope according to:

$$\frac{\int \text{ROI}(t')dt'}{\text{ROI}(T)} = \text{DVR} \left[ \frac{\left( \int \text{OCC}(t')dt' + \frac{\text{OCC}(T)}{k_2'} \right)}{\text{ROI}(T)} \right] + \text{intercept}. \quad \text{Eq. 2}$$

where the average  $K_2'$  value from a reference region (i.e., cerebellum or occipital cortex) can be applied without requiring the plasma input function (23). Because of an inability to measure plasma input function accurately after 40 min, we implemented graphical analysis using the following steps:

1. We assumed that the reference region does not have an irreversible binding. The plasma input function was acquired in 10 subjects (5 normal, 5 Parkinson's disease patients) up to 25 min postinjection in 4 patients, 40 min in 4 subjects and 65 min in 2 subjects. This does not provide an adequate plasma input function to analyze striatal kinetic data for a 100-min scan period. Because the slope in the first equation became linear by 3–5 min postinjection in the occipital region, we could calculate DV and  $k_2'$  using each plasma input function. To analyze striatal kinetic data for a 100-min scan period, we estimated the plasma integral after the last point of the metabolite analysis through the end of the study by the linear extrapolation of Equation 1. Ideally, this extrapolation would be done on the arterial time-activity curve. However, the noise in most plasma curves prevented an accurate extrapolation using this method. Therefore, the extrapolation was performed using the plot for the occipital region only. This can be justified based on the fact that the occipital region is assumed to have no DAT binding, and the plot for this region reached linearity within 10 min. The extrapolated plasma curve thus obtained was then applied for the striatal region where the linearity was reached, in some cases, only after 40 min postinjection. The parameters DV and DVR were calculated both for the striatum and extrastriatal regions in these 10 subjects. The  $K_1$  value can be approximated from slope/intercept in Equation 1. The efflux parameter  $k_2'$  is simply the inverse of the intercept.
2. We used Equation 2 to estimate DVR by using the average  $k_2'$  value obtained in the occipital region (23). DVR values estimated with and without plasma input function ( $\text{DVR}_{\text{plasma}}$  and  $\text{DVR}_{\text{ref}}$ , respectively) were compared in the 10 subjects described earlier. The values of  $\text{DVR}_{\text{ref}}$  were obtained for both the caudate and putamen. Subsequently, we calculated  $\text{DVR}_{\text{ref}}$  to investigate pathophysiological correlations in the group of normal subjects ( $n = 7$ ) and in Parkinson's disease patients ( $n = 10$ ).

### Ratio Method

To assess the clinical use of a simple single-scan acquisition, we measured the ratio of the caudate and putamen to occipital radioactivity in a single 8-min frame beginning at 90 min postinjection ( $\text{SOR}_{90 \text{ min}}$ ).  $\text{SOR}_{90 \text{ min}}$  was compared with  $\text{DVR}_{\text{ref}}$  by computing the Pearson product-moment correlation coefficients.

### Clinical Correlations

**Normal Aging.** In the normal subjects, we correlated subject age with the mean of the left and right values for  $\text{DVR}_{\text{ref}}$  and  $\text{SOR}_{90 \text{ min}}$  by computing the Pearson product-moment correlation coefficients.

**Disease Discrimination.** Discriminant analysis for the Parkinson's disease patients and normal subjects was performed for  $\text{DVR}_{\text{ref}}$  and  $\text{SOR}_{90 \text{ min}}$  using a stepwise procedure with the F-test associated with Wilk's  $\lambda$ . We also used age-corrected  $\text{DVR}_{\text{ref}}$  based on the results of normal aging described above. Age-corrected  $\text{DVR}_{\text{ref}}$  was expressed as the ratio of age-expected control values. The discriminant analysis were performed by using putaminal  $\text{DVR}_{\text{ref}}$  and  $\text{SOR}_{90 \text{ min}}$  contralateral to the symptomatic limbs. This analysis was restricted to the Parkinson's disease patients with early disease (H&Y Stages I and II) and the normal controls.

**Disease Severity Assessment.** In the Parkinson's disease group, we independently correlated the mean left and right values of  $\text{DVR}_{\text{ref}}$  and  $\text{SOR}_{90 \text{ min}}$  with UPDRS motor rating scores by computing the Pearson moment correlation coefficients.

## RESULTS

### Plasma Analysis

A representative HPLC analysis of arterial plasma after [ $^{18}\text{F}$ ]-FPCIT administration is given in Figure 1. The recovery of the radioactivity in the supernatant was 50%–60%. Plasma  $^{18}\text{F}$  activity peaked within 2 min after the start of injection (mean at peak:  $0.0076 \pm 0.0042\%$   $^{18}\text{F}$ /injected dose/ml) and decreased rapidly by 10 min postinjection ( $0.0012 \pm 0.0004\%$   $^{18}\text{F}$ /injected dose/ml) (Fig. 2). Plasma  $^{18}\text{F}$  was constant thereafter except for the marginal increase between 25 and 40 min. In the HPLC, the acetonitrile-extractable fraction displayed two distinct peaks. The fraction of unmetabolized [ $^{18}\text{F}$ ]-FPCIT in arterial plasma decreased rapidly after the injection ( $57\% \pm 18\%$  at 5 min;  $43\% \pm 14\%$  at 10 min;  $23\% \pm 11\%$  at 25 min postinjection; Fig. 2A). The major arterial plasma radiolabeled fraction was considered a polar metabolite (21), which increased rapidly in an inverse manner to the time-course of the unmetabolized [ $^{18}\text{F}$ ]-FPCIT. Because of the low  $^{18}\text{F}$  activity of HPLC samples taken after 25 min, the unmetabolized [ $^{18}\text{F}$ ]-FPCIT could be reliably quantified after this point in only 6 subjects. On the other hand, the peak corresponding to a polar metabolite was consistently detected. We noted significant variability in the clearance of the unmetabolized [ $^{18}\text{F}$ ]-FPCIT reflecting intersubject differences of over twofold in the rate constants for the washout of the parent tracer. Figure 2B illustrates an example of a plasma input function obtained by the two exponential fit applied to the parent fraction.

### Brain Uptake

Figure 3 shows PET images obtained in a normal volunteer and in two Parkinson's disease patients. Representative time-activity curves of selected brain regions from a normal volunteer and a Parkinson's disease patient are shown in Figures 4A and B, respectively. In the control group, striatal radioactivity rapidly increased with time and became relatively constant from 40 min onwards ( $0.02\% \pm 0.01\%$  dose/g for both in caudate and putamen at peak activity). In the normal volunteers, the ratio of striatum to occipital (SOR) was  $3.65 \pm 0.34$  (mean  $\pm$  s.d.) in caudate nucleus, and  $3.35 \pm 0.17$  in putamen at 90 min

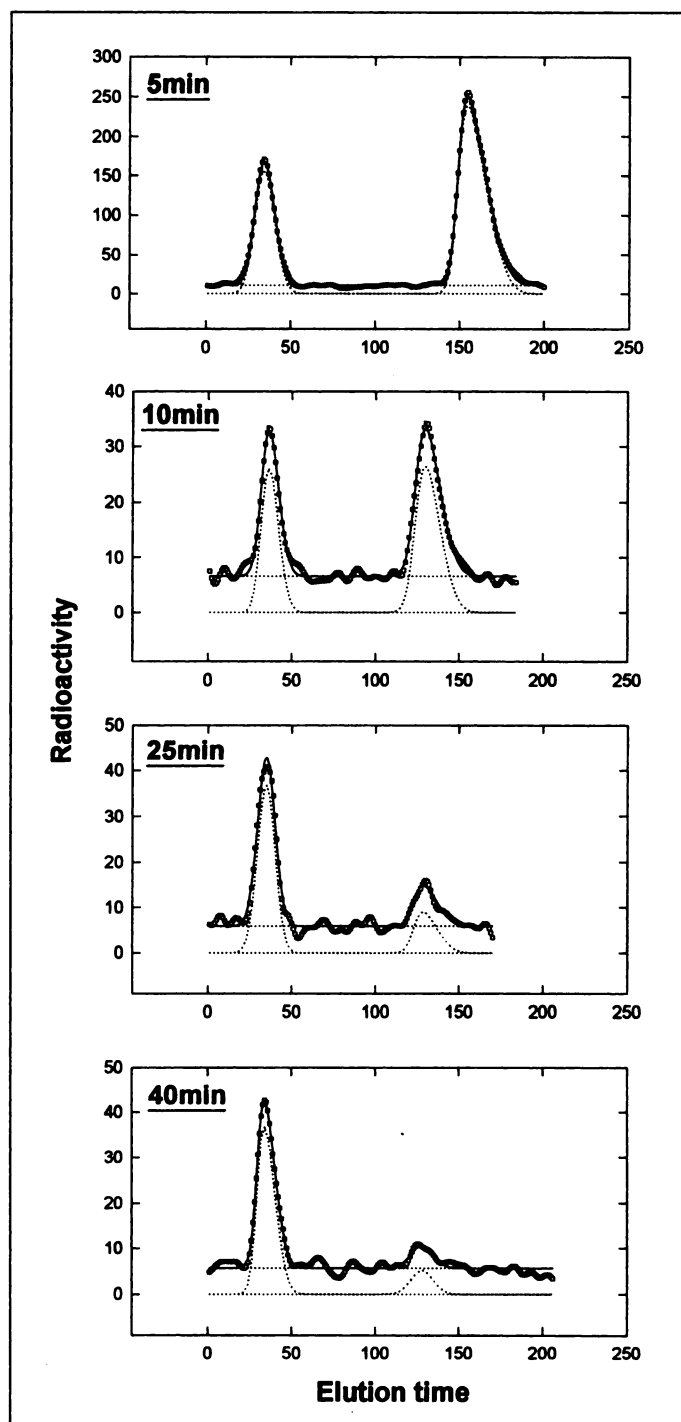


**FIGURE 1.** Plasma high-performance liquid chromatography obtained at 5, 10, 25 and 40 min postinjection. Second peak represents unmetabolized [ $^{18}\text{F}$ ]-FPCIT.

postinjection. In the Parkinson's disease patients, putaminal radioactivity peaked within 30 min and showed a gradual clearance. There was moderate uptake in the thalamus and the midbrain in all likelihood reflecting modest serotonergic binding in these regions. At 90 min postinjection, radioactivity in the thalamus and the midbrain was higher than in cortex (thalamus; 1.4–1, midbrain; 1.7–1). Occipital activity showed a peak at 15 min and washed out at a rate of approximately 50%/hr. The dynamic radioactivity data were similar across the cortical regions and the cerebellum.

When radioactivity in the occipital cortex was subtracted from that in striatum, the time curves for specific striatal uptake reached a plateau phase in the Parkinson's disease patients (Fig.

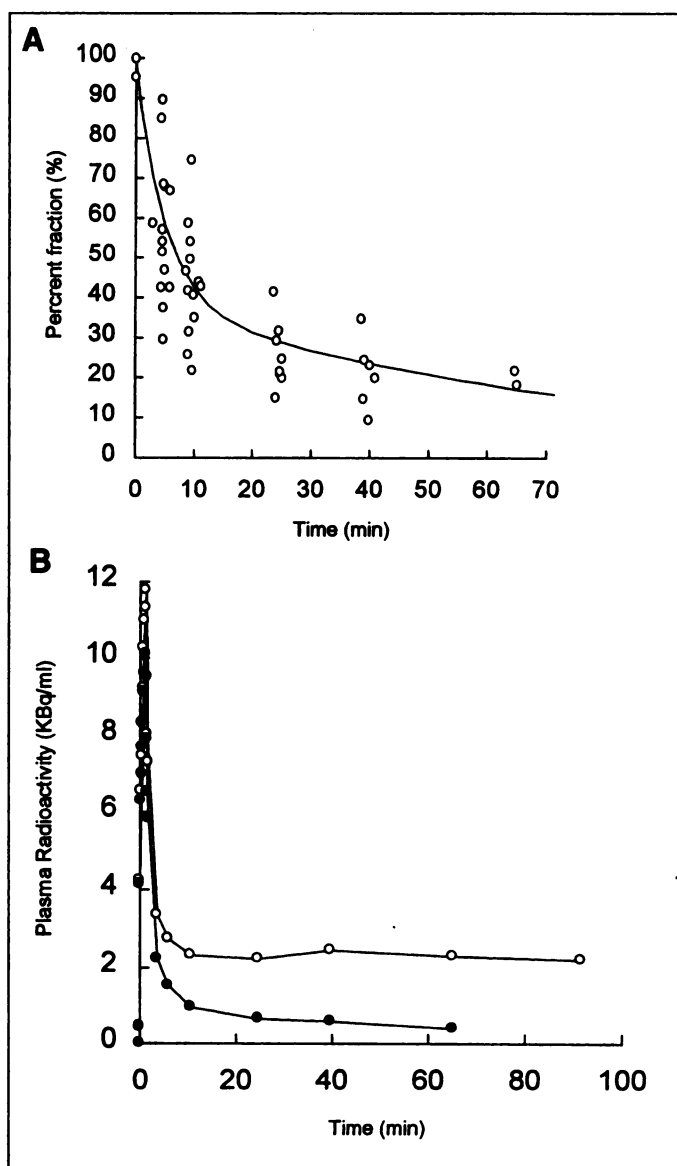


**FIGURE 2.** (A) Fraction of unmetabolized [ $^{18}\text{F}$ ]-FPCIT by high-performance liquid chromatography. Data at 40 and 65 min consisted of 6 and 2 subjects, respectively. Line was obtained by double exponential fit to all data points. (B) Arterial input function for [ $^{18}\text{F}$ ]-FPCIT. Plasma  $^{18}\text{F}$  (open circles) and unmetabolized [ $^{18}\text{F}$ ]-FPCIT (filled circles).

5A). The specific uptake did not reach plateau completely in three of the normal subjects for the duration of the scan. The ratio of striatum to occipital radioactivity increased linearly or curvilinearly over 100 min (Fig. 5B).

#### Graphical Method

The slope of  $\int \text{ROI}(t')dt'/\text{ROI}(T)$  versus  $\int \text{Cp}(t')dt'/\text{ROI}(T)$  in occipital cortex reached linearity by 3–5 min postinjection. Figure 6A represents two examples of Logan plots in which the occipital slope was determined by the plasma input function acquired 0–25 min and 0–65 min, respectively. The results of graphical analysis are presented in Table 2. The average DV and  $k'_2$  in occipital were  $9.8 \pm 2.6$  ml/g and  $0.037 \pm 0.009$   $\text{min}^{-1}$ , respectively, giving an estimated occipital  $K_1$  value of  $0.35 \pm 0.01$  ml/min/ml. Plasma integral after the point of the last metabolite analysis was subsequently calculated by Equation 1. The slope of  $\int \text{ROI}(t')dt'/\text{ROI}(T)$  versus  $\int \text{Cp}(t')dt'/\text{ROI}(T)$  using data of striatum and extrastriatal regions became linear by 5 min postinjection and remained linear thereafter (Fig. 6A). We thus included all data points between 5 and 100

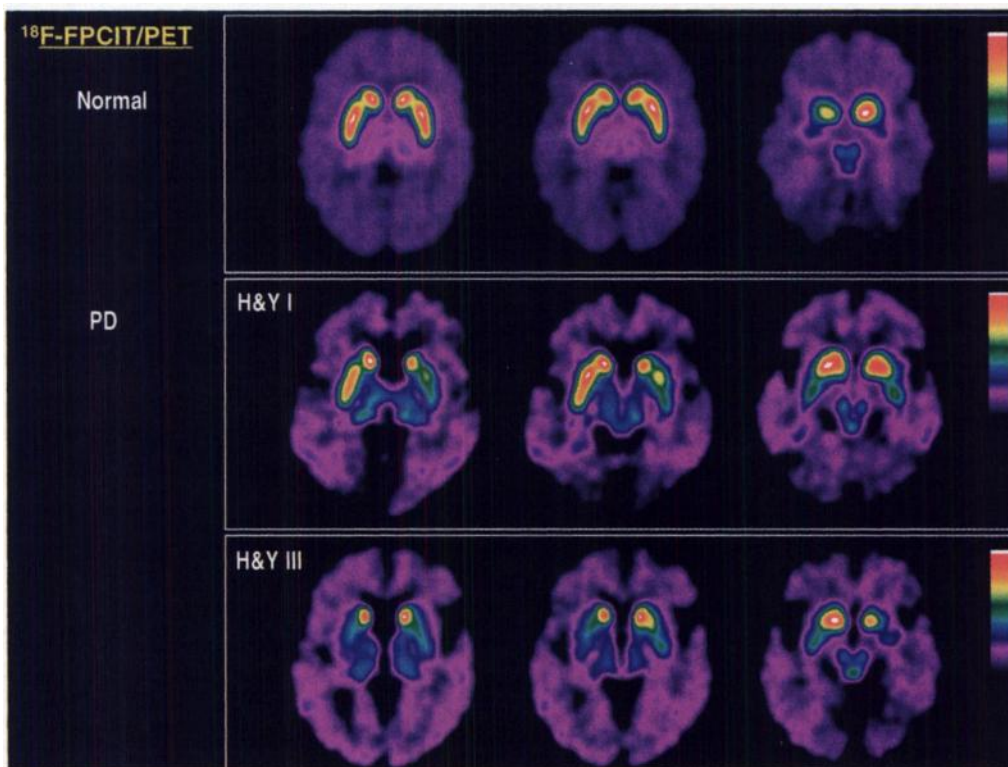


**FIGURE 3.** PET images obtained with [ $^{18}\text{F}$ ]-FPCIT in normal volunteer (top), in Patient 5 with H&Y Stage I Parkinson's disease (middle) and in Patient 10 with H&Y Stage III Parkinson's disease (bottom). Caudate and putamen were well resolved in all cases. Decrease in tracer uptake in Parkinson's disease patients is evident in posterior putamen. This reduction was most pronounced contralaterally in early-stage patient with asymmetrical clinical involvement; it was symmetrically reduced in more advanced patients. Modest uptake in midbrain corresponded to substantia nigra, locus coeruleus or aqueductal gray.

min in the regression. The results of graphical method in striatum and extrastriatal regions are listed in Table 2. In normal subjects ( $n = 5$ ; age range 23–70; mean 44.6 yr), the average  $K_1$  estimates for caudate and putamen were  $0.43 \pm 0.10$  and  $0.42 \pm 0.09$ , respectively. In Parkinson's disease ( $n = 5$ ; age range 47–75; mean 63.0 yr), the  $K_1$  estimates for caudate and putamen were  $0.31 \pm 0.07$  and  $0.32 \pm 0.07$ , respectively.

For caudate and putamen, the slope of  $\int \text{ROI} (t') dt' / \text{ROI} (T)$  versus  $\int \text{OCC}(t') dt' + \text{OCC} (T) / k_2' / \text{ROI} (T)$  in caudate and putamen reached linearity in approximately 10–30 min postinjection (Fig. 6B). Thus, the initial time for slope calculation was set at 30 min postinjection (Fig. 6B). The relationship of  $\text{DVR}_{\text{plasma}}$  and  $\text{DVR}_{\text{ref}}$  was linear with a slope of 0.98 ( $r = 0.98$ ,  $p < 0.0001$ ;  $n = 10$ ) (Fig. 7A). There was also a significant correlation between  $\text{DVR}_{\text{ref}}$  and  $\text{SOR}_{90 \text{ min}}$  with a slope of 0.61 ( $r = 0.93$ ,  $p < 0.0001$ ;  $n = 17$ ) (Fig. 7B).  $\text{SOR}_{90 \text{ min}}$  underestimated DVR significantly in the range of high DAT binding.

### Clinical Correlations

**Normal Aging.** We found a significant age-dependent decline in  $\text{DVR}_{\text{ref}}$  both in caudate and putamen (caudate:  $r = 0.87$ ,  $p < 0.02$ ; putamen:  $r = 0.96$ ,  $p < 0.001$ ). This decline corresponds to approximately 7.7% and 6.4% reduction in caudate and putamen per decade (Fig. 8). We also found a significant age-dependent decline in  $\text{SOR}_{90 \text{ min}}$  both in caudate and putamen (caudate:  $r = 0.85$ ,  $p < 0.02$ ; putamen:  $r = 0.79$ ,  $p < 0.04$ ).

**Disease Discrimination.** In early-stage Parkinson's disease patients, both DVR and  $\text{SOR}_{90 \text{ min}}$  values contralateral to the symptomatic side were significantly reduced in both the caudate and putamen compared with normal volunteers (caudate:  $p < 0.0005$ ; putamen:  $p < 0.0001$ ; two-tailed Student's  $t$ -test; Fig. 9). Additionally, in the H&Y Stage I patients, ipsilateral DVR and  $\text{SOR}_{90 \text{ min}}$  ("preclinical striatum") was reduced in caudate and putamen, albeit to a lesser degree in caudate (caudate:  $p < 0.05$ ; putamen:  $p < 0.0005$ ; two-tailed Student's  $t$ -test).

Both  $\text{DVR}_{\text{ref}}$  and  $\text{SOR}_{90 \text{ min}}$  contralateral to the symptomatic limbs side significantly discriminated the two subject groups (F

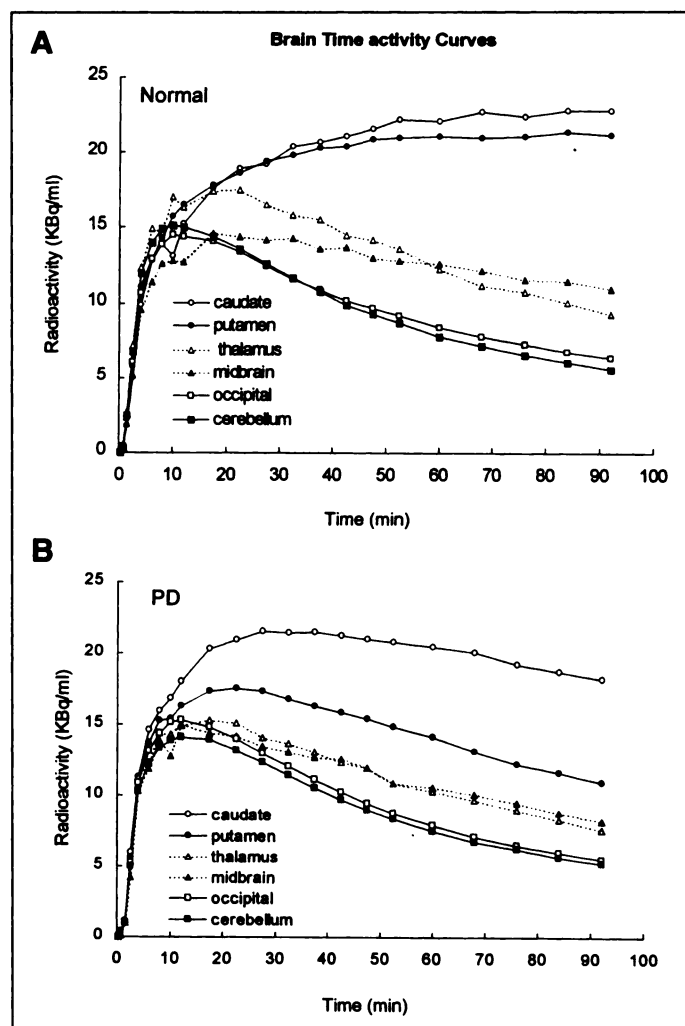


**FIGURE 4.** Time-activity curves for [ $^{18}\text{F}$ ]-FPCIT in (A) normal subject and (B) patient with Parkinson's disease. Activity is expressed as KBq per cc of tissue.

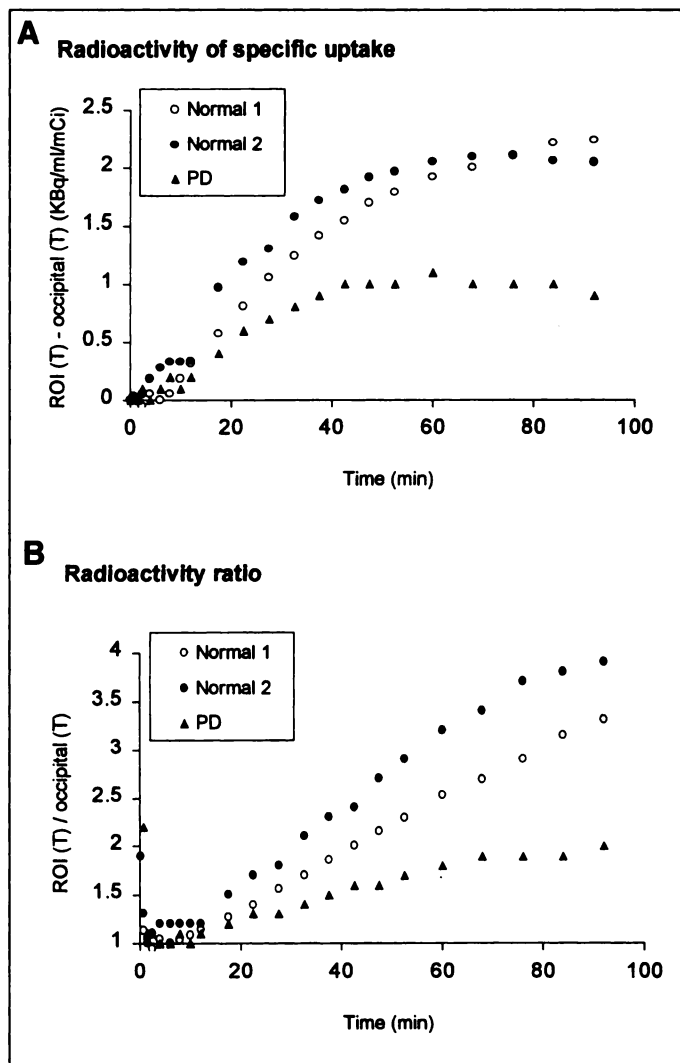


**FIGURE 5.** (A) Putamen specific uptake and (B) ratio in Parkinson's disease patient and in 2 normal volunteers. Specific uptake reached plateau at approximately 60 min in Parkinson's disease patient and in 1 normal subject. By contrast, specific uptake did not reach plateau in other normal subject. Radioactivity ratio increased even after specific uptake had reached plateau.

(1,23) = 72.4, 91.6,  $p < 0.0001$  for  $DVR_{ref}$  and  $SOR_{90\ min}$ , respectively). Age-corrected  $DVR_{ref}$  afforded comparatively better discrimination accuracy ( $F(1,23) = 139.1$ ,  $p < 0.0001$ ) than the corresponding age-uncorrected  $DVR_{ref}$  values. A discriminant line based on age-corrected  $DVR_{ref}$  correctly classified all H&Y Stage I and II patients.

In early stage patients, contralateral  $DVR_{ref}$  values were reduced to 81% and 58% of age-expected control values for caudate and putamen, respectively. Ipsilateral  $DVR_{ref}$  values (preclinical striatum in H&Y Stage I patients) were reduced to 88% and 67% of age-expected  $DVR_{ref}$  for caudate and putamen, respectively.

**Disease Severity Assessment.** Age-corrected  $DVR_{ref}$  correlated significantly with composite UPDRS scores ( $r = -0.66$ ,  $p < 0.05$ ,  $n = 10$ ). This correlation remained significant even when the analysis was restricted to H&Y Stage I and II patients ( $r = -0.69$ ,  $p < 0.05$ ,  $n = 9$ ). Both  $SOR_{90\ min}$  and age-uncorrected  $DVR_{ref}$  showed trends in correlations with composite UPDRS ratings ( $SOR_{90\ min}$ :  $r = -0.57$ ;  $DVR_{ref}$ :  $r = -0.58$ ,  $p = 0.08$  for both correlations).

## DISCUSSION

In this article, we present the quantitative results of human PET studies using [ $^{18}F$ ]-FPCIT for assessing striatal dopamine

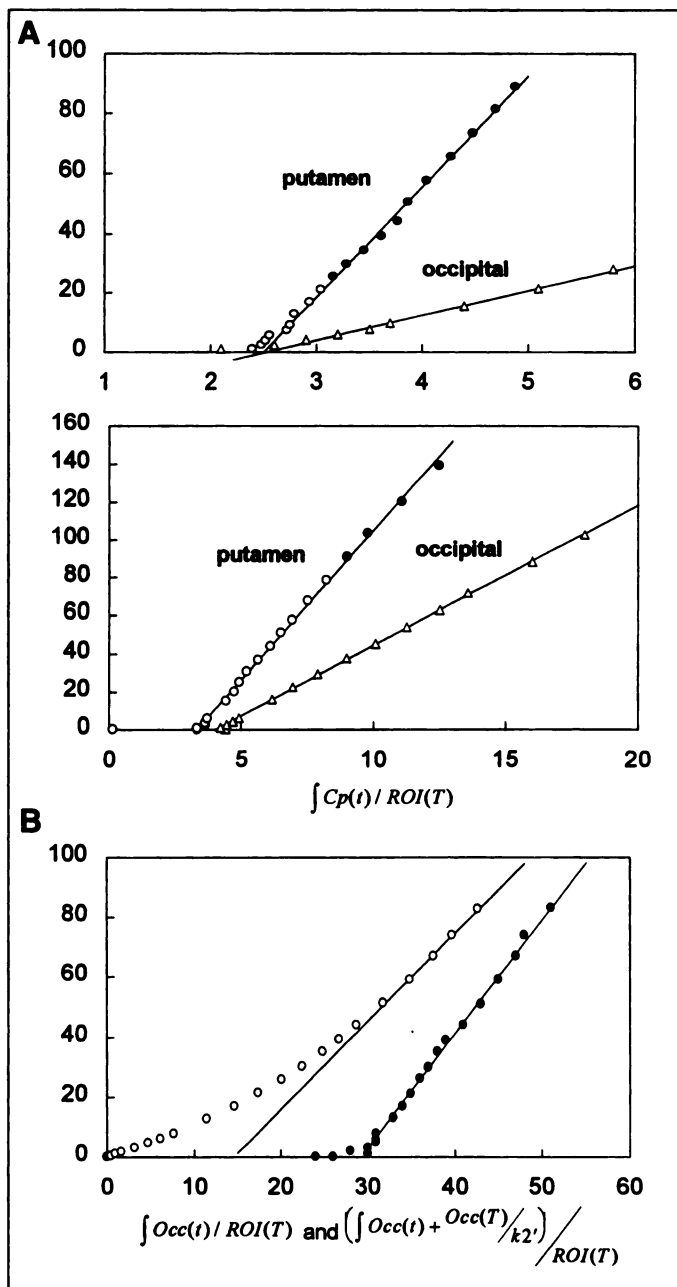


**FIGURE 6.** (A) Graphical analysis in putamen (circles) and occipital cortex (triangles). Filled circles indicate data points obtained from calculated plasma integral by using linear extrapolation for occipital cortex. Plasma input function was available for 0–25 min (upper panel) and 0–65 min (bottom panel). (B) Striatal  $\int ROI(t')dt'/ROI(T)$  was plotted against either  $\int OCC(t')dt'/ROI(T)$  (open circle) or  $(\int OCC(t')dt' + OCC(T)/k_2')/ROI(T)$  (filled circle). The average  $k_2$  for occipital cortex was used ( $k_2 = 0.037\ min^{-1}$ ).

transporter binding. Our studies revealed that this tracer has a high target-to-background ratio with the characteristics of a high affinity reversible ligand. As in our early SPECT studies using radioiodinated FPCIT (9), these PET experiments with [ $^{18}F$ ]-FPCIT/PET demonstrate a significant decline of striatal tracer uptake with age in normal subjects. In addition, there was a remarkable reduction in striatal [ $^{18}F$ ]-FPCIT binding in Parkinson's disease patients at the earliest stages of illness, which is correlated with independent rating of disease severity. These results indicate that [ $^{18}F$ ]-FPCIT and PET may be used to quantify presynaptic dopaminergic function in living subjects.

## Plasma Metabolite Analysis

In contrast to the presence of multiple metabolites with [ $^{11}C$ ]- and [ $^{123}I$ ]-labeled FPCIT, HPLC chromatograms for [ $^{18}F$ ]-

**TABLE 2**  
Regional Fluorine-18-FPCIT Transport and Uptake

	Normal (n = 5; age range 23–70 yr; mean 44.6 yr)			Parkinson's disease (n = 5; age range 47–75 yr; mean 63.0 yr)			Total (n = 10)	
	K <sub>1</sub> (ml/min/g)	DV* (ml/g)	DVR†	K <sub>1</sub> (ml/min/g)	DV (ml/g)	DVR	K <sub>1</sub> (ml/min/g)	DV (ml/g)
Caudate	0.43 (0.10)	45.7 (15.6)	4.32 (1.03)	0.31 (0.07)	23.9 (6.3)	2.73 (0.55)	–	–
Putamen	0.42 (0.09)	40.5 (14.2)	3.79 (0.73)	0.32 (0.07)	16.5 (4.5)	1.89 (0.29)	–	–
Thalamus	0.47 (0.11)	15.4 (4.4)	1.44 (0.10)	0.34 (0.10)	11.9 (2.6)	1.36 (0.06)	–	–
Midbrain	0.36 (0.07)	18.7 (5.2)	1.75 (0.22)	0.30 (0.08)	12.8 (3.1)	1.46 (0.11)	–	–
Cerebellum	0.48 (0.10)	9.6 (3.0)	0.90 (0.15)	0.34 (0.10)	8.1 (2.4)	0.92 (0.14)	0.41 (0.10)	8.8 (2.7)
Occipital	0.40 (0.08)	10.7 (3.1)	–	0.31 (0.10)	8.8 (1.8)	–	0.35 (0.10)	9.8 (2.6)

\*DV = distribution volume from Equation 1.

†DVR = DV<sub>ROI</sub>/DV<sub>occipital</sub> calculated using Equation 1.

Numbers in parentheses are s.d.

FPCIT indicated the presence of a single metabolite (1,13,28). As described previously (21), we believe that the metabolite is the [<sup>18</sup>F]-FPCIT free carboxylic acid form (an aqueous form), which is generated by the enzymatic hydrolysis of the 2β-methyl ester of the parent compound. Our finding is in keeping with the data previously obtained with fluorinated 2β-carbomethoxy-3β-(4-chlorophenyl)-8-(-3-fluoropropyl) nortropane in animal experiments (29). The fraction of [<sup>18</sup>F]-FPCIT rapidly decreased to a level of 25% after 25 min postinjection with marked intersubject variability in the rate of clearance. In addition, because of the low radioactivity of HPLC samples, it was not always possible to quantify the fraction of parent compound after 25 min postinjection. The recovery of the radioactivity in the supernatant was approximately 50%–60% in this study. Because this study confirmed the absence of lipophilic metabolites, ether extraction may be useful for generating the plasma input function in future studies (29).

### Characteristics of Brain Uptake

A high target-to-background ratio (3.5:1 at 90 min) in striatum is compatible with the in vivo affinity described with this ligand (2). Assuming a putaminal blood flow of 0.65 ml/g/min, the mean putaminal K<sub>1</sub> estimates extraction fraction as 0.65 with a permeability surface product of 1.04 ml/g/min. This suggests that [<sup>18</sup>F]-FPCIT has a high membrane permeability. The tracer uptake in the neocortical regions and the cerebellum was equivalent, which suggested low in vivo affinity for the cortical DAT and the 5HT reuptake sites. The tracer uptake in thalamus is smaller than that of β-CIT, which is compatible with the reported differences in DAT selectivity (2,12,30).

Our estimation of DV and k<sub>2</sub>' involved an assumption of linearity of the slope of Equation 1 up to 100 min even though the plasma data were available only for 25, 40 or 65 min. For the occipital cortex, the slope of the line was observed to be linear from 5–25 min in all cases. Once the linearity was fully established, we extended this line to 100 min based on the assumed consistency of the FPCIT exchange process for the duration of the study. Figure 7 lends support to this assumption where we observe a high correlation between DVR based on plasma data (with the assumption of extended linearity) versus that calculated from Equation 2 where no such assumption was made. Moreover, the value of k<sub>2</sub>' is not expected to change for different study duration.

The displacement study performed by using [O-Methyl <sup>11</sup>C] FPCIT suggested that the striatal FPCIT binding is specific for the dopamine transporters and reversible (1). When ROI

(T)/occipital (T) in striatum was plotted against ∫ Occipital (t')dt'/occipital (T), we noted a progressive decline in the slope, suggesting reversible tracer binding (data not shown). The striatal dynamic radioactivity showed linearity by 5 min postinjection when ∫ ROI(t')dt'/ROI(T) was plotted against ∫ Cp (t')dt'/ROI (T). This indirectly indicates that the specific binding is rapid compared to the ligand transport. Recently, several methods have been proposed for a modification of graphical analysis without requiring arterial blood sampling (23,31). In keeping with these studies, we observed that the slope becomes effectively constant after 30–40 min when ∫ ROI(t') dt'/ROI(T) was plotted against either ∫ Occ (t') dt'/ROI(T) or (∫ Occ (t') dt' + Occ(T)/k<sub>2</sub>')/ROI (T). However, because the ratio of striatum to occipital significantly increased with time, the slope obtained without including Occ (T)/k<sub>2</sub>' term in linear regression resulted in the significant underestimation of DVR. In keeping with the data of Logan et al. (23), the correspondence between DVR determined with and without plasma input function is sufficiently close (r = 0.98) as to allow image quantification using the noninvasive approach.

On the other hand, an apparent time dependency was demonstrated in the relationship between the simple radioactivity ratio measured at 90 min and DVR. In the high end of the range of DAT bindings, SOR measured at 90 min significantly underestimated DVR. Thus, the application of peak equilibrium analysis would require the extension of data acquisition for 3–5 hr in some cases (2,13). Nonetheless, the long half-life of <sup>18</sup>F permits delayed scanning up to 6 hr. However, as explained in the previous studies, because specific and nonspecific regions do not reach equilibrium simultaneously, the ratio of tissue radioactivity at the transient equilibrium state generally overestimates DVR (23,32). In [<sup>18</sup>F]-FPCIT studies, because of the slow washout from the striatum, the striatal to occipital radioactivity ratio increases even after the specific uptake reached a plateau phase (Fig. 5). In practice, the timing of transient equilibrium may not be determined with sufficient accuracy to calculate V<sub>3</sub>', and the advantage of measuring the regional radioactivity ratio at longer time points postinjection over the graphical method remains to be seen (22,23). Besides the lack of true equilibrium, other disadvantages of SOR include its dependence on blood flow, blood-brain permeability and peripheral tracer clearance. At the same time, SOR has the distinct advantage of not requiring dynamic scanning thereby reducing the scan duration as well as patient discomfort. In addition, computer data storage needs for a single static scan is minimal compared to dynamic scan data.

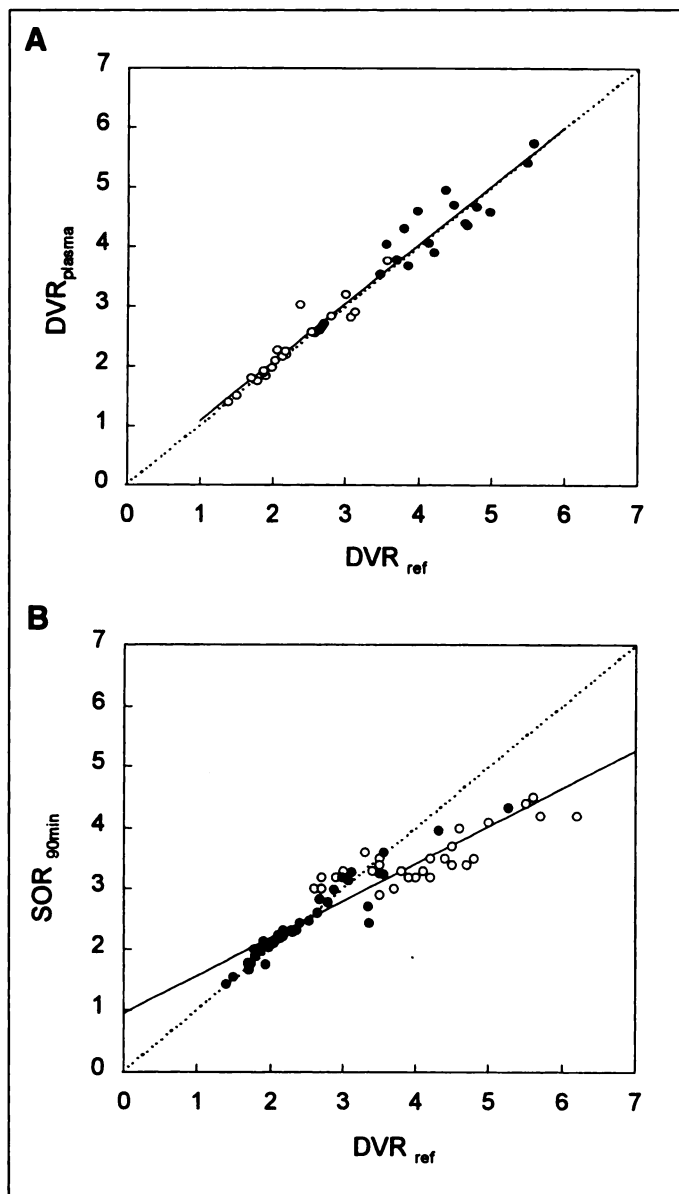


**FIGURE 7.** (A) Linear correlation between striatal DVR calculated with either plasma input function ( $DVR_{plasma}$ ) or average  $k_2'$  value in occipital cortex ( $DVR_{ref}$ ) for caudate and putamen in 10 subjects. Regression equation is  $DVR_{plasma} = 0.98 \cdot DVR_{ref} + 0.10$  ( $r = 0.98$ ,  $p < 0.0001$ ). (B) Comparison of  $SOR_{90min}$  and  $DVR_{ref}$  for caudate and putamen in 17 subjects. There is consistent underestimation in  $SOR$  for subjects with high DAT binding. Regression equation is  $SOR_{90min} = 0.61 \cdot DVR_{ref} + 0.96$  ( $r = 0.93$ ,  $p < 0.0001$ ). Filled circles = Parkinson's disease subjects; open circles = normal subjects. Dotted line represents line of identity.

### Clinical Correlations

Despite the limited sample size investigated, we confirmed an age-related decline in the striatal DAT binding in normal subjects. This finding is in keeping with the postmortem studies demonstrating a 4.7% decrease of nigral neurons (33) as well as approximately 10% decline of the striatal dopamine transporter binding (34). The rate of 6%–7% decline per decade is in agreement with findings previously reported by SPECT and PET studies using DAT imaging tracers ( $[^{11}C]$ -cocaine: 7.0%,  $[^{11}C]$ -d-threo-methamphetamine: 6.6% (6,35);  $[^{123}I]$ - $\beta$ -CIT: 8% (15);  $[^{123}I]$ -FPCIT: 3.3% (9)).

Both DV and DVR are approximately half their values in Parkinson's disease patients compared to normal subjects (Table 2). The parameter DV is available only for a subset of the total number of subjects and is associated with almost twice the coefficient-of-variation compared to DVR. We, therefore, limit

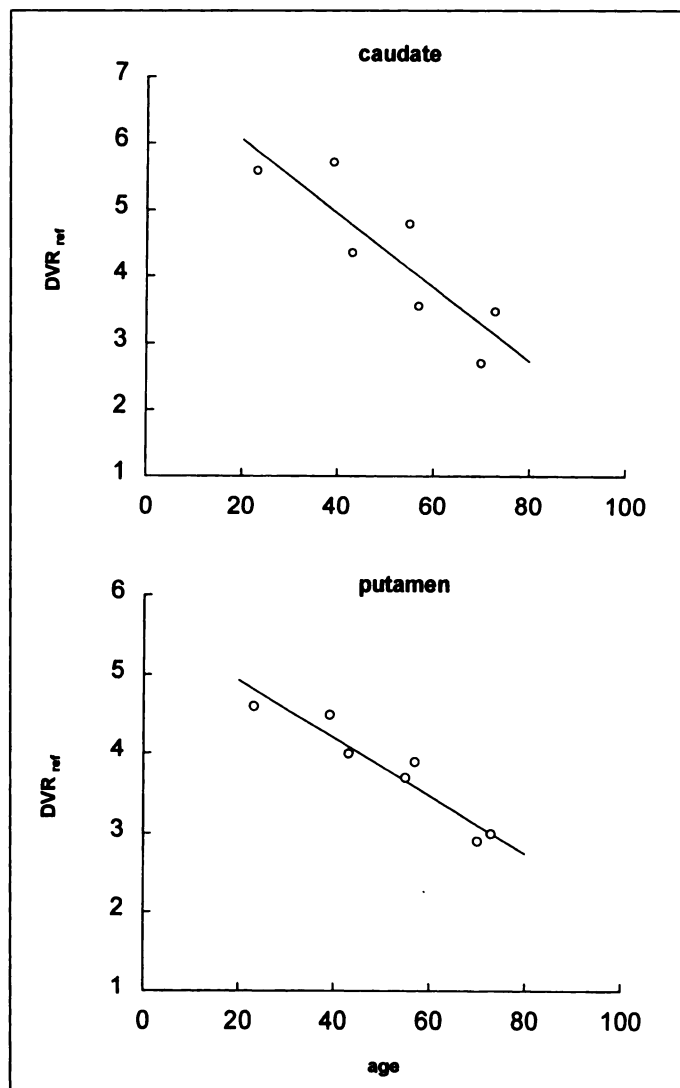


**FIGURE 8.** Striatal  $[^{18}F]$ -FPCIT binding (DVR) versus age in seven normal volunteers. Caudate:  $DVR = -0.055 \cdot age + 7.15$ ;  $r = 0.87$ ;  $p < 0.02$ . Putamen:  $DVR = -0.036 \cdot age + 5.66$ ;  $r = 0.96$ ;  $p < 0.001$ .

our discussion to DVR. DVR accurately discriminated early-stage Parkinson's disease patients from normal subjects. Although  $SOR_{90min}$  underestimated specific binding to a larger extent in normal subjects, similar findings also were obtained by this parameter. We note that the discriminant functions obtained here must be further validated with prospective imaging studies. Nonetheless, our results indicate that a single-frame acquisition after 90 min can be used for clinical diagnostic purposes. Indeed, we have observed that an 8 min, three-dimensional frame at 90–100 min postinjection provided sufficient image quality for regional measurements. Scans of longer duration can be used also to enhance significant signal-to-noise ratio. Although the patient population in this study was somewhat older than the normal controls, we note that age-corrected and age-uncorrected DVR provided a degree of discrimination comparable to that obtained with SPECT imaging using  $[^{123}I]$ -FPCIT and  $[^{123}I]$ - $\beta$ -CIT (9,36). Nonetheless, the small number of subjects in the SPECT and PET imaging studies does not warrant a detailed comparison of the two tracers.

Our  $[^{18}F]$ -FPCIT studies revealed decrements in DAT binding in the contralateral putamen in early-stage Parkinson's disease, suggesting that a reduction of approximately 40% may be necessary to produce motor signs in this disorder. On the

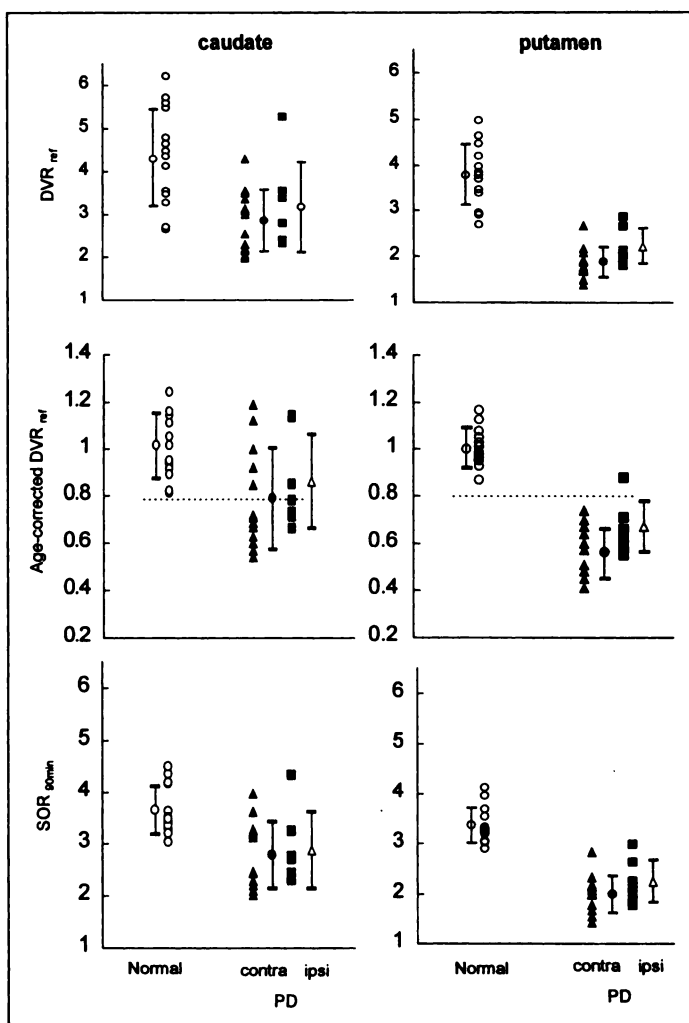


**FIGURE 9.** Discriminant analysis of early-stage Parkinson's disease patients and normal subjects using DVR (top), age-corrected DVR (middle) and  $SOR_{30min}$  (bottom). Significant between-group separation was obtained with all these parameters ( $p < 0.0001$ ). When  $DVR_{ref}$  was corrected by age-expected control values, discriminant line (dots) completely detected all normal subjects and Parkinson's disease patients. Open circles = mean bilateral normal values; filled triangles = values contralateral to the affected limbs in early-stage Parkinson's disease patients (H&Y Stage I and II); filled squares = ipsilateral values (preclinical striatum) in unilaterally involved Parkinson's disease patients (H&Y Stage I).

other hand, the average of DAT reduction in presymptomatic side was approximately 30%. The magnitude of these reductions are in keeping with results of other dopaminergic imaging studies using tracers for DAT or DDC activity (37,38). Indeed, the significant decrease in binding obtained in both symptomatic and presymptomatic striata suggests the potential use of this agent in the early detection of parkinsonism.

## CONCLUSION

Fluorine-18-FPCIT is a high-affinity tracer with a striatum-to-occipital ratio of 3:4 for normal subjects. The plasma metabolite analysis revealed the presence of a single polar metabolite, which could simplify kinetic modeling. However, a rapid clearance of the parent fraction precluded the accurate measurements of plasma input function. Regional distribution volume ratios estimated using graphical analysis without blood sampling might be suitable for the quantification of DAT activity. An age-related decline in DAT binding was observed in normal subjects. Significant bilateral reductions in putaminal DAT binding were evident in Parkinson's disease patients, which correlated with the degree of motor impairment. These

findings confirmed our prior results obtained using [ $^{123}$ I]-FPCIT with SPECT. Our data support the use of FPCIT as an objective marker for diagnosing and assessing parkinsonism at its earliest clinical stages using either PET or SPECT imaging modalities.

## ACKNOWLEDGMENTS

This work was supported by NIH grant NSRO135069 and the National Parkinson Foundation. Dr. Ken Kazumata is supported by the Veola Kerr Fellowship of the Parkinson Disease Foundation. Dr. Angelo Antonini is a faculty fellow of the Parkinson Disease Foundation and the United Parkinson Foundation. Dr. David Eidelberg is supported by the Cotzias Fellowship of the American Parkinson Disease Association. We thank Dr. Robert Dahl and Mr. Ralph Mattachieri for cyclotron support and Drs. John Kabebian and Gilles Tamagnan of Research Biochemicals Inc. for providing the nor  $\beta$ -CIT precursor.

## REFERENCES

- Lundkvist C, Halldin C, Swahn CG, et al. [O-Methyl- $^{11}C$ ]  $\beta$ -CIT-FP, a potential radioligand for quantitation of the dopamine transporter: preparation, autoradiography, metabolite studies, and positron emission tomography examinations. *Nucl Med Biol* 1995;22:7:905-913.
- Abi-Dargham A, Gendelman MS, DeErasquin GA, et al. SPECT imaging of dopamine transporters in human brain with iodine-123-fluoroalkyl analogs of  $\beta$ -CIT. *J Nucl Med* 1996;37:1129-1133.
- Kaufmann MJ, Madras BK. Severe depletion of cocaine recognition sites associated with the dopamine transporter in Parkinson's disease striatum. *Synapse* 1991;49:43-49.
- Niznik HB, Fogel EF, Fassos FF, et al. The dopamine transporter is absent in parkinsonian putamen and reduced in the caudate nucleus. *J Neurochem* 1991;56:192-198.
- Frost JJ, Rosier AJ, Reich SG, et al. Positron emission tomographic imaging of the dopamine transporter with  $^{11}C$ -WIN 35,428 reveals marked declines in mild Parkinson's disease. *Ann Neurol* 1993;34:423-431.
- Laruelle M, Baldwin RM, Malison RT, et al. SPECT imaging of dopamine and serotonin transporters with [ $^{123}$ I]  $\beta$ -CIT: pharmacological characterization of brain uptake in nonhuman primates. *Synapse* 1993;13:295-309.
- Volkow ND, Fowler JS, Wang GJ, et al. Decreased dopamine transporters with age in healthy human subjects. *Ann Neurol* 1994;36:237-239.
- Volkow ND, Ding YS, Fowler JS, et al. New PET ligand for the dopamine transporter: studies in the human brain. *J Nucl Med* 1995;36:2162-2168.
- Ishikawa T, Dhawan V, Kazumata K, et al. Comparative nigrostriatal dopaminergic imaging with iodine-123- $\beta$ -CIT-FP/SPECT and fluorine-18-FDOPA/PET. *J Nucl Med* 1996;37:1760-1765.
- Laihinne AO, Rinne JO, Kjell A, et al. PET studies on brain monoamine transporters with carbon-11- $\beta$ -CIT in Parkinson's disease. *J Nucl Med* 1995;36:1263-1267.
- Neumeyer JL, Wang S, Gao Y, et al. N- $\omega$ -fluoroalkyl analogs of (1R)-2b-carbomethoxy-3b-(4-iodophenyl)-tropane ( $\beta$ -CIT): radiotracer for PET and SPECT imaging of the dopamine transporters. *J Med Chem* 1994;37:1558-1561.
- Baldwin RM, Zea-Ponce Y, Zoghbi S, et al. Evaluation of the monoamine uptake site ligand [ $^{123}$ I]methyl 3 $\beta$ -(4-iodophenyl)-tropane-2b-carboxylate ([ $^{123}$ I] $\beta$ -CIT) in non-human primates: pharmacokinetics, biodistribution and SPECT brain imaging coregistered with MRI. *Nucl Med Biol* 1993;20: 597-606.
- Baldwin RM, Zea-Ponce Y, Al-Tikriti MS, et al. Regional brain uptake and pharmacokinetics of [ $^{123}$ I] N- $\omega$ -2b-carboxy-3b-(4-iodophenyl)-nortropane esters in baboons. *Nucl Med Biol* 1995;22:211-219.
- Kuikka JT, Bergstrom KA, Ahonen A, et al. Comparison of iodine-123-labeled 2 $\beta$ -carboxymethoxy-3 $\beta$ -(4-iodophenyl) tropane and 2 $\beta$ -carboxymethoxy-3 $\beta$ -(4-iodophenyl)-N-(3-fluoropropyl) nortropane for imaging of the dopamine transporter in the living human brain. *Eur J Nucl Med* 1995;22:356-360.
- van Dyck CH, Seibyl JP, Malison RT, et al. Age-related decline in striatal dopamine transporter binding with iodine-123- $\beta$ -CIT SPECT. *J Nucl Med* 1995;36:1175-1181.
- Eidelberg D, Takikawa S, Dhawan V, et al. Striatal 18F-DOPA uptake: absence of aging effect. *J Cereb Blood Flow Metab* 1993;13:881-888.
- Kish SJ, Zhong XH, Hornykiewicz O, et al. Striatal DOPA decarboxylase in aging: disparity between postmortem and PET studies? *Ann Neurol* 1995;38:260-264.
- Dhawan V, Ishikawa T, Patlak C, et al. Combined FDOPA and 3OMD PET studies in Parkinson's disease. *J Nucl Med* 1996;37:209-216.
- Ishikawa T, Dhawan V, Chaly T, et al. The clinical significance of dopa decarboxylase activity in Parkinson's disease. *J Nucl Med* 1996;37:216-222.
- Ishikawa T, Dhawan V, Chaly T, et al. Fluorodopa PET with an inhibitor of Catechol-O-methyltransferase: effect of the plasma 3-O-methyldopa fraction on data analysis. *J Cereb Blood Flow Metab* 1996;16:854-863.
- Chaly T, Dhawan V, Kazumata K, et al. Radiosynthesis of [ $^{18}F$ ] N-3-fluoropropyl-2- $\beta$ -carboxymethoxy-3- $\beta$ -(4-iodophenyl) nortropane and the first human study with PET. *Nucl Med Biol* 1996;23:999-1004.
- Logan J, Fowler JS, Volkow ND, et al. Graphical analysis of reversible radioligand binding from time-activity measurements applied to [ $^{11}C$ -methyl]-(-)-cocaine PET studies in human subjects. *J Cereb Blood Flow Metab* 1990;10:740-747.
- Logan J, Fowler JS, Volkow ND, et al. Distribution volume ratio without blood sampling from graphical analysis of PET data. *J Cereb Blood Flow Metab* 1996;16: 834-840.

24. Fahn S, Elton RL and the UPDRS development committee. Unified Parkinson's disease rating scale. In: Fahn S, Marsden CD, Calne D, Goldstein M, eds. *Recent developments in Parkinson's disease*, vol. 2. Floral Park, NJ: Macmillan; 1987:293-304.
25. DeGrado TR, Turkington TG, Williams JJ, et al. Performance characteristics of a whole-body PET scanner. *J Nucl Med* 1994;35:1398-1406.
26. Hariz MI. Clinical study on the accuracy of the Laitinen CT-guidance system in functional stereotactic neurosurgery. *Stereotact Funct Neurosurg* 1991;56:109-128.
27. Dhawan V, Jarden JO, Strother S, et al. Effect of blood curve smearing on the accuracy of parameter estimates obtained for  $^{82}\text{Rb}$ /PET studies of blood-brain-barrier permeability. *Phys Med Biol* 1988;33:61-74.
28. Bergstrom KA, Halldin C, Lundkvist C, et al. Characterization of  $^{11}\text{C}$  or  $^{123}\text{I}$  labeled  $\beta\text{-FP-CIT}$  and  $\beta\text{-CIT-FE}$  metabolism measured in monkey and human plasma. Identification of two-labeled metabolites with HPLC. *Hum Psychopharmacol* 1996;11:483-490.
29. Goodman MM, Keil R, Shoup TM, et al. Fluorine-18-FPCT: a PET radiotracer for imaging dopamine transporters. *J Nucl Med* 1997;38:119-126.
30. Kessler RM, Whetsell WO, Ansari MS, et al. Identification of extrastriatal dopamine D2 receptors in postmortem human brain with [ $^{125}\text{I}$ ]-epidepride. *Brain Res* 1993;609:237-243.
31. Ichise M, Ballinger JR, Golan H, et al. Noninvasive quantification of dopamine D2 receptors with iodine-123-IBF SPECT. *J Nucl Med* 1996;37:513-520.
32. Carson RE, Channing MA, Blasberg RG, et al. Comparison of bolus and infusion methods for receptor quantitation: application to [ $^{18}\text{F}$ ]-cyclofoxy and PET. *J Cereb Blood Flow Metab* 1993;13:24-42.
33. Fearnley JM, Lees AJ. Aging. Parkinson's disease: substantia nigra regional selectivity. *Brain* 1991;114:2283-2301.
34. De Keyser JD, Ebinger G, Vauquelin G. Age-related changes in the human nigrostriatal dopaminergic system. *Ann Neurol* 1990;27:157-161.
35. Volkow ND, Ding YS, Fowler JS, et al. Dopamine transporters decrease with age. *J Nucl Med* 1996;37:554-559.
36. Seibyl JP, Marek KL, Quinlan D, et al. Decreased SPECT [ $^{123}\text{I}$ ]  $\beta\text{-CIT}$  striatal uptake correlates with symptom severity in Parkinson's disease. *Ann Neurol* 1995;38:589-598.
37. Brooks DJ, Ibanez V, Sawle GV, et al. Differing patterns of striatal  $^{18}\text{F}$ -dopa uptake in Parkinson's disease, multiple system atrophy and progressive supranuclear palsy. *Ann Neurol* 1990;28:547-555.
38. Marek KL, Seibyl JP, Zoghbi SS, et al. Iodine-123  $\beta\text{-CIT}$ /SPECT imaging demonstrates bilateral loss of dopamine transporters in hemi-Parkinson's disease. *Neurology* 1996;46:231-237.

## FIRST IMPRESSIONS Duplicated Heart?

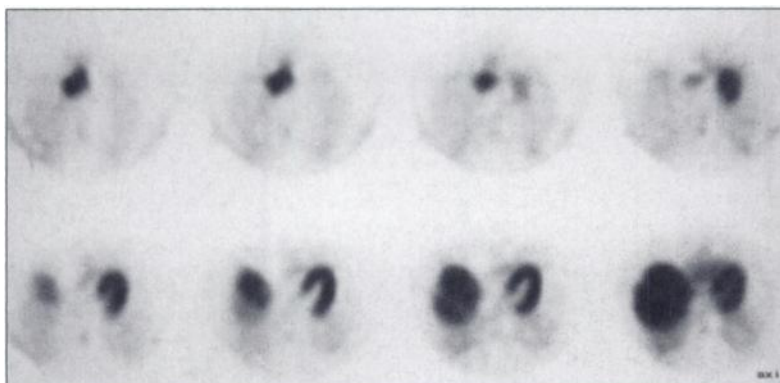


**Figure 1.**

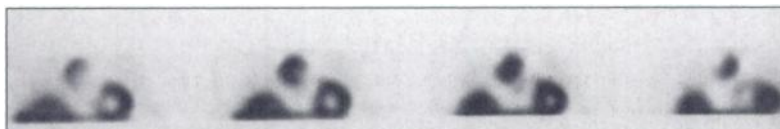


**Figure 2.**

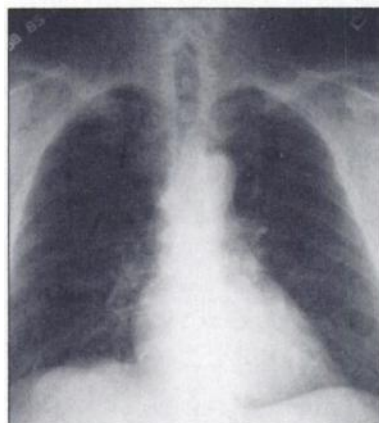


**Figure 3.**

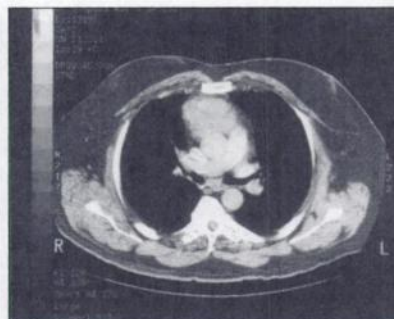


**Figure 4.**

### PURPOSE

A 53-yr-old man was evaluated for recurrent chest pain using myocardial perfusion imaging with  $^{99\text{m}}\text{Tc-MIBI}$ . Images obtained during stress demonstrated a large focus of intense, abnormal activity located in the mediastinum, superior to the heart (Figs. 1 and 2). A chest x-ray was normal (Fig. 3). Because of the findings on the myocardial scan, the patient had a CT scan that demonstrated a large soft-tissue mass in the anterior mediastinum (Fig. 4). Biopsy revealed a malignant thymoma.

### TRACER

Technetium-99m-MIBI (8 mCi)

### ROUTE OF ADMINISTRATION

Intravenous, at peak exercise during standard treadmill exercise test

### TIME AFTER INJECTION

Exercise continued for 90 sec; images were obtained 15 min later

### INSTRUMENTATION

Prism 3000 SPECT camera (Picker) with low-energy, high-resolution collimators

### CONTRIBUTORS

Amanda Moser, Alan Siegel, Robert Dallas, Dartmouth-Hitchcock Medical Center, Lebanon, NH